

Excitation of Helium by Electron Impact*

Victor Franco

Physics Department, Brooklyn College of the City University of New York, Brooklyn, New York 11210

(Received 12 March 1973)

Excitation of helium atoms by electron impact is studied for intermediate- and high-energy electrons. Calculations of the differential cross sections for the $1S-2^1S$ transition are made by use of a one-dimensional integral representation of the scattering amplitude obtained in the Glauber approximation. Comparisons with the Born approximation and with measurements between 22 and 600 eV are presented. Several sets of ground-state and excited-state wave functions are used. The results are a distinct improvement over the Born approximation at all energies considered and are in good agreement with the measurements above ~ 90 eV. At lower energies the Glauber predictions reproduce the qualitative features of the data. The results also show that the more-general one-dimensional integral expression for charged-particle-atom scattering amplitudes, derived earlier, can be used to perform calculations with relative ease.

I. INTRODUCTION

It is often assumed that at large impact energies the electron-excitation cross sections for atoms are given accurately by the first Born approximation. Such assumptions are often encouraged by comparisons of calculations with measurements of *integrated* cross sections. We have pointed out¹ that such comparisons may be quite deceiving since the integrated cross section is only a single number and does not reveal as much detailed information about the reaction mechanisms as do differential cross sections. Furthermore, examples have been presented^{2,3} in which two theories yield virtually identical integrated cross sections over a large energy range but predict strikingly different angular distributions. It is clear that tests and comparisons of scattering theories should be made with differential cross sections in preference to integrated cross sections whenever possible.

Although there have been many measurements of inelastic electron-helium integrated (i.e., total) cross sections, until recently there has been little work on absolute differential-cross-section measurements of e -He elastic and inelastic scattering. However, within the past few years rather detailed measurements of differential cross sections for e -He elastic scattering have been made, for example, by Vriens, Kuyatt, and Mielczarek,⁴ by Chamberlain, Mielczarek, and Kuyatt,⁵ and by Bromberg.⁶ Extensive measurements of the differential cross sections for the $1S-2^1S$ transition in e -He collisions at 500 eV were made by Lassetre, Krasnow, and Silverman,⁷ by Silverman and Lassetre,⁷ and by Skerbele and Lassetre.⁸ These have recently been supplemented by the corresponding measurements of Vriens, Simpson, and Mielczarek⁹ for electrons

between 100 and 400 eV, of Chamberlain, Mielczarek, and Kuyatt⁵ for electrons between 50 and 400 eV, of Rice, Truhlar, Cartwright, and Trajmar¹⁰ for electrons between 26 and 82 eV, of Opal and Beaty¹¹ at 82 and 200 eV, and of Crooks and Rudd¹² at 50 and 100 eV.

This recent flurry of experimental activity has been accompanied by no less an effort on the theory of the calculations for electron-helium collisions. For inelastic scattering the most widely used theory at high impact energies has been the first Born approximation. The extensive and highly accurate calculations of Kim and Inokuti¹³ and of Bell, Kennedy, and Kingston¹³ on the oscillator strengths of the helium atom deserve mention for their great use in testing the Born approximation. Lassetre¹⁴ has observed that in the range 300–500 eV the Born approximation does not hold when term symbols are the same in the initial and final states, as is the case with the $1S-2^1S$ transition of helium. Consequently, reliance upon the Born approximation for such transitions, even at high impact energies, is unjustified.

Some time ago we applied the Glauber approximation¹⁵ to scattering of charged particles by hydrogen atoms,² and we predicted the angular distributions for elastic scattering of electrons between 100 eV and 5 keV. These predictions were confirmed by subsequent measurements.¹⁶ Since that time there have been numerous applications of the method to elastic and inelastic scattering of electrons and protons by hydrogen atoms.^{3,17-19} All the above calculations contain *no adjustable parameters*. These analyses yield results which are, for the most part, in rather good agreement with the existing data. They also point out that the first Born approximation is unreliable below ~ 500 eV for electrons and below

~500 keV for protons when such quantities as angular distributions are required.

Recently the theory has been extended to scattering of charged particles by helium atoms.¹ In that work explicit applications to elastic scattering of electrons were also made, and comparisons with the Born approximation and with data between 100 and 500 eV were presented. Both the magnitudes and the shapes of the scattering intensities obtained in the Born approximation were in rather gross disagreement with the measurements. On the other hand, the Glauber approximation yielded angular distributions whose shapes were in excellent agreement with the measurements and whose magnitudes were within ~20% of the data at the higher energies and ~35% of the data at the lower energies. The only freedom in the calculations was the choice of the helium ground-state wave function. A simple wave function with modest accuracy was used. A more accurate wave function would not have changed the qualitative conclusions, although the quantitative results may have been altered somewhat (perhaps for the better).

In Ref. 1 the scattering amplitude was reduced from an eight-dimensional integral to a three-dimensional integral. Although such a reduction is substantial, numerical evaluation of the three-dimensional integral requires significant time. Recently a calculation of the 1S-2¹S transition in helium was published by Yates and Tenney²⁰ who showed that the three-dimensional integral can be reduced further to a two-dimensional integral. However, an even greater reduction had been previously made by the author,²¹ a reduction which applies not only to helium atoms but to more complex atoms as well. We showed that if the product of the initial state (*i*) and final state (*f*) wave functions can be expressed as

$$\varphi_f^* \varphi_i = \sum_{k=0}^N \left(c_k \prod_{j=1}^Z [r_{j,k,j}^n e^{-\alpha_{k,j} r_j} \times Y_{l_j m_j}(\theta_j, \phi_j) Y_{l_j' m_j'}(\theta_j, \phi_j)] \right), \quad (1.1)$$

where r_j, θ_j, ϕ_j are the spherical coordinates of the *j*th electron and Y_{lm} are normalized spherical harmonics, then the scattering amplitude F_{fi} can be expressed as a *one-dimensional* integral. In the present work we demonstrate the utility and

ease of application of this one-dimensional integral by using it to calculate the 1S-2¹S transition in helium. The analysis is applied in detail to electrons with incident energies between 22 and 600 eV and the results are compared with the data.

The present work differs in spirit from that of Ref. 20 in that it is a detailed application of a very general method for describing collisions of charged particles with arbitrary atoms to the particular case of 1S-2¹S transitions of helium. It should dispel any impressions to the effect that the general method is cumbersome and impractical, and should answer any doubts regarding the numerical tractability of the method. In addition, we have considered in this work all the available data in the comparisons of theory with experiment. We have included the high-*q* data at 100 and 200 eV where the calculations and measurements go out to squared momentum transfers of $q^2 \approx 50$ for the first time. These cases clearly show the superiority of the Glauber theory and are also important because similar experiments at and above 200 eV are now being carried out.

The numerical results appear to be quite consistent with those of Ref. 20, although exact comparisons cannot be made since different sets of wave functions have been used. The present method has the advantage over that of Ref. 20 in that it requires evaluation of only a one-dimensional integral rather than of a two-dimensional integral, and is applicable to arbitrary atoms.

In Sec. II we apply the more general expression for the scattering amplitude derived in Ref. 21 to the 1S-2¹S transition in helium. In Sec. III we very briefly discuss the first Born approximation. In Sec. IV we present the results of our calculations and compare them with measurements.

II. REDUCTION OF SCATTERING AMPLITUDE FOR 1S-2¹S TRANSITION IN HELIUM

Let $F_{fi}(q)$ be the amplitude for collisions in which helium undergoes a transition from an initial state *i* with wave function φ_i to a final state *f* with wave function φ_f , and in which the incident particle imparts a momentum $\hbar \vec{q}$ to the target. If the product $\varphi_f^* \varphi_i$ is of the form given by Eq. (1.1), then the scattering amplitude is given by Eq. (24) of Ref. 21. For an incident momentum $\hbar \vec{k}$, we have²¹

$$F_{fi}(\vec{q}) = -ik e^{iM(\phi_q + \pi/2)} \int_0^\infty db J_M(qb) b \sum_k c_k \prod_j \sum_{L_j} A_{L_j} \times \sum_p D_p E(\eta) b^{3+n_{k,j}} \left[\left(\frac{\partial}{\partial \gamma} \right)^{1+n_{k,j}-2p-M_j} I(M_j, \gamma) \right]_{\gamma=\alpha_{k,j} b/2}, \quad (2.1)$$

where

$$I(M_j, \gamma) = 2^{-2i\eta} \sum_w G_w [\gamma^{-2i\eta} - 2^p - 2 E_1(\eta) {}_1F_2(M_j + w - i\eta; w - 2p - i\eta, M_j + 1; \gamma^2) \\ + \gamma^{2p - 2w} E_2(\eta) {}_1F_2(M_j + 2p + 1; 2 + M_j + 2p - w + i\eta, 2p + 2 - w + i\eta; \gamma^2)]. \quad (2.2)$$

In Eq. (2.2), E , G_w , E_1 , and E_2 are given by

$$E(\eta) = -\pi 2^{1+2i\eta} \Gamma(1 + i\eta) / \Gamma(1 - i\eta), \quad (2.3)$$

$$G_w = \frac{1}{4} i\eta [(M_j + p)! (-p)_w]^2 (-1)^w / [M_j! (M_j + 1)_w w!], \quad (2.4)$$

$$E_1(\eta) = \Gamma(M_j + w - i\eta) \Gamma(2p + 1 - w + i\eta) / [(M_j + 2p)! M_j!], \quad (2.5)$$

$$E_2(\eta) = \Gamma(w - 2p - 1 - i\eta) / \Gamma(2 + M_j + 2p - w + i\eta), \quad (2.6)$$

where the symbol $(a)_n$ is Pochhammer's symbol defined by $(a)_n = \Gamma(a + n) / \Gamma(a)$. Also $\eta = Z'e^2 / \hbar v$, where $Z'e$ is the charge of the incident particle and v is its initial speed in the laboratory system.

Equation (2.1) may look discouragingly complicated. However, for particular transitions simplifications generally occur. For example, if $\varphi_f \varphi_i$ is spherically symmetric (as it is for the $1S-2^1S$ transition we are considering), then

$$l_j = l'_j = m_j = m'_j = L_j = M = p = M_j = 0,$$

$$A_0 = 1/4\pi, \quad G_0 = \frac{1}{4} i\eta,$$

$$D_0 = -(-\frac{1}{2})^{n_k, j}.$$

Equation (2.1) then reduces to a much simpler-looking form given by

$$F_{fi}(q) = -ik \int_0^\infty db J_0(qb) b \sum_k c_k \\ \times \prod_j \frac{-1}{4\pi} (-\frac{1}{2})^{n_k, j} E(\eta) b^{3+n_k, j} \\ \times \left[\left(\frac{\partial}{\partial \gamma} \right)^{1+n_k, j} I(0, \gamma) \right]_{\gamma = \alpha_{k, j} b^{1/2}}, \quad (2.7)$$

where

$$I(0, \gamma) = i\eta 2^{-2i\eta} [\gamma^{-2i\eta} E_1(\eta) \\ \times I_0(2\gamma) + E_2(\eta) \\ \times {}_1F_2(1; 2 + i\eta, 2 + i\eta; \gamma^2)], \quad (2.8)$$

$$F_{fi}(q) = -\frac{1}{4} ik 2^{2i\eta} \frac{\Gamma^2(1 + i\eta)}{\Gamma^2(1 - i\eta)} \sum_{k=1}^8 c_k (-\frac{1}{2})^{n_k} \int_0^\infty b^{7+n_k} J_0(qb) db \left(\frac{\partial}{\partial \gamma} I(0, \gamma) \right)_{\gamma = \alpha_{k, 1} b^{1/2}} \\ \times \left[\left(\frac{\partial}{\partial \gamma} \right)^{1+n_k} I(0, \gamma) \right]_{\gamma = \alpha_{k, 2} b^{1/2}}. \quad (2.13)$$

If we define

$$\alpha_k = c_k / 32 N_i^2 N_f^2, \quad (2.14)$$

with

$$E_1(\eta) = \Gamma(-i\eta) \Gamma(1 + i\eta) \quad (2.9)$$

and

$$E_2(\eta) = \Gamma(-1 - i\eta) / \Gamma(2 + i\eta). \quad (2.10)$$

In Eq. (2.8) we have used the identity

$${}_1F_2(-i\eta; -i\eta, 1; \gamma^2) = {}_0F_1(1; \gamma^2) \\ = I_0(2\gamma),$$

where I_0 is the modified Bessel function.

To obtain an explicit expression for the integrand in Eq. (2.7) we need explicit forms for $\varphi_f \varphi_i$. For the helium ground-state wave function we take

$$\varphi_i(\vec{r}_1, \vec{r}_2) = (N_i^2 / \pi) (e^{-Z_1 r_1} + c e^{-Z_2 r_1}) \\ \times (e^{-Z_1 r_2} + c e^{-Z_2 r_2}). \quad (2.11)$$

For the 2^1S state wave function, we take

$$\varphi_f(\vec{r}_1, \vec{r}_2) = (N_f^2 / \pi) \\ \times [e^{-2r_1} (e^{-Z_3 r_2} - c' \gamma_2 e^{-Z_4 r_2}) \\ + e^{-2r_2} (e^{-Z_3 r_1} - c' \gamma_1 e^{-Z_4 r_1})]. \quad (2.12)$$

All lengths are expressed in atomic units (i.e., in units of $a_0 = \hbar^2 / m_e e^2$).

If we take advantage of the symmetry with respect to interchange of coordinates in the integrand of the original expression for $F_{fi}(\vec{q})$, given by Eq. (3) of Ref. 21, the amplitude for $1S-2^1S$ transitions simplifies to

Table I lists the values of the parameters appearing in Eq. (2.13) in terms of parameters in the wave functions φ_i and φ_f given by Eqs. (2.11)

and (2.12).

To reduce Eq. (2.13) to final form requires a bit of straightforward algebra. The result we obtain is

$$F_{fi}(q) = -2ikN_i^2 N_f^2 \left(\sum_{k=1}^4 a_k \int_0^\infty b^7 J_0(qb) \mathfrak{A}(\frac{1}{2}\alpha_{k,1}b, \eta) \mathfrak{B}(\frac{1}{2}\alpha_{k,2}b, \eta) db - \frac{1}{2} \sum_{k=5}^8 a_k \int_0^\infty b^8 J_0(qb) \right. \\ \left. \times \mathfrak{C}(\frac{1}{2}\alpha_{k,1}b, \eta) \mathfrak{D}(\frac{1}{2}\alpha_{k,2}b, \eta) db \right), \quad (2.15)$$

where

$$\mathfrak{A}(\gamma, \eta) = \Gamma^2(1+i\eta)\gamma^{-2i\eta-3}[\gamma I_1(2\gamma) - (1+i\eta)I_0(2\gamma)] \\ - \gamma {}_1F_2(2; 3+i\eta, 3+i\eta; \gamma^2)/[(1+i\eta)(2+i\eta)]^2 \quad (2.16)$$

and

$$\mathfrak{B}(\gamma, \eta) = \Gamma^2(1+i\eta)\gamma^{-2i\eta-4}[(1+i\eta)(3+i\eta)I_0(2\gamma) - (3+4i\eta)\gamma I_1(2\gamma) + 2\gamma^2 I_2(2\gamma)] \\ - \left({}_1F_2(2; 3+i\eta, 3+i\eta; \gamma^2) + \frac{4\gamma^2 {}_1F_2(3; 4+i\eta, 4+i\eta; \gamma^2)}{(3+i\eta)^2} \right) / [(1+i\eta)(2+i\eta)]^2. \quad (2.17)$$

We note that the only function that depends on q is $J_0(qb)$ and the only functions that depend on the incident energy (other than trivial algebraic functions) are $\Gamma(1+i\eta)$, ${}_1F_2(2; 3+i\eta, 3+i\eta; \gamma^2)$, and ${}_1F_2(3; 4+i\eta, 4+i\eta; \gamma^2)$. Consequently numerical calculations of Eq. (2.15) may be done for a wide range of angles (i.e., of q) and of energies (i.e., of η) without having to recompute the Bessel, γ , and hypergeometric functions very often.

The differential cross section for excitation from state i to state f is given by

$$\frac{d\sigma_{fi}}{d\Omega} = \frac{k'}{k} |F_{fi}(q)|^2, \quad (2.18)$$

where $\hbar k'$ is the momentum of the scattered electron and is determined from energy conservation.

III. BORN APPROXIMATION

Our numerical results will be compared with the Born approximation and the data. The Born amplitude for the $1S - 2^1S$ transition may be written in the form

$$F_{fi}^B(q) = -\frac{2m}{\hbar^2} \int_0^\infty \frac{\sin qr}{qr} V_{fi}(r) r^2 dr, \quad (3.1)$$

where

$$V_{fi}(r) = -e^2 \int \left(\frac{2}{r} - \frac{1}{|\vec{r} - \vec{r}_1|} - \frac{1}{|\vec{r} - \vec{r}_2|} \right) \\ \times \varphi_f^*(\vec{r}_1, \vec{r}_2) \varphi_i(\vec{r}_1, \vec{r}_2) d\vec{r}_1 d\vec{r}_2. \quad (3.2)$$

We note that the orthogonality of the initial- and final-state wave functions results in *zero* contribution to V_{fi} from the interaction between the incident electron and the target protons. The expression for F_{fi} derived in Sec. II therefore

differs from the Born amplitude in that it explicitly treats the interaction of the incident electron with the target protons.² Furthermore, the first term in the expansion of F_{fi} , as given by Eq. (2.1), in powers of η yields the first Born approximation.

A straightforward calculation of Eqs. (3.1) and (3.2) with the wave functions of Eqs. (2.11) and (2.12) yields the Born amplitude.

IV. RESULTS AND DISCUSSION

In this section are presented the results of our computations which are compared with the corresponding measurements between 22 and 600 eV. At each energy considered we show the results of the present calculations and of the Born approximation for each of three pairs of initial- and final-state wave functions.

The initial-state wave functions have the form given by Eq. (2.11). The final-state wave functions have the form given by Eq. (2.12). For each set of initial- and final-state wave functions, φ_i and φ_f are orthonormal and contain eight parameters

TABLE I. Values of parameters appearing in expressions for the scattering amplitude F_{fi} , given in terms of parameters of the wave functions φ_i and φ_f .

k	a_k	n_k	$\alpha_{k,1}$	$\alpha_{k,2}$
1	1	0	$2+Z_1$	Z_1+Z_3
2	c	0	$2+Z_1$	Z_2+Z_3
3	c	0	$2+Z_2$	Z_1+Z_3
4	c^2	0	$2+Z_2$	Z_2+Z_3
5	$-c'$	1	$2+Z_1$	Z_1+Z_4
6	$-cc'$	1	$2+Z_1$	Z_2+Z_4
7	$-cc'$	1	$2+Z_2$	Z_1+Z_4
8	$-c^2c'$	1	$2+Z_2$	Z_2+Z_4

N_i^2 , Z_1 , Z_2 , c , N_f^2 , Z_3 , Z_4 , and c' , not all of which are independent. The values used for these parameters are listed in Table II for each of the three pairs of wave functions. In no case is the overlap integral greater than 4×10^{-6} in magnitude.

The first pair of wave functions, the parameters of which are given in the first row of Table II, were obtained by using for φ_i the variational wave function calculated by Löwdin.²² This wave function is a fairly good analytical fit to the Hartree self-consistent-field function for the helium ground state. For φ_f we used a slightly modified version of the 2^1S -state wave function of Marriott and Seaton,²³ namely, one in which the value of c' was chosen to ensure that this state be orthogonal to the ground state. This set of wave functions and results obtained with them will be denoted by LMS.

The second pair of wave functions, the parameters of which are given in the second row of Table II, were obtained by using for φ_i a simple but very accurate fit (found by Byron and Joachain²⁴) to the Hartree-Fock wave function of Roothaan *et al.*²⁵ For φ_f we used a slightly modified version (obtained by Van den Bos²⁶) of the 2^1S -state wave function of Marriott and Seaton. The modification made by Van den Bos ensured the orthogonality of φ_i and φ_f . This set of wave functions and the results obtained with them will be denoted by BJB.

The third pair of wave functions, the parameters of which are given in the third row of Table II, were obtained by using for φ_i the wave function of Byron and Joachain.²⁴ For φ_f we used the fit (obtained by Flannery²⁷) to the unrestricted Hartree-Fock function of Cohen and McEachran.²⁸ This fit was made with the condition that the 2^1S wave function be orthogonal to the $1S$ wave function of Ref. 24. The above set of wave functions (φ_i from Ref. 24 and φ_f from Ref. 27) and the results obtained with them will be denoted by BJF.

We have compared our Born results with the accurate results of Kim and Inokuti¹³ and of Bell *et al.*¹³ All three pairs of wave functions are in good qualitative agreement in the range $10^{-2} \leq (\alpha^2 q^2) \leq 10^2$. In this range the generalized oscillator strength varies by more than five orders of magnitude. In this range the largest deviations from the accurate results occur with the BJF wave functions (~ 20 – 35%). The smallest deviations occur with the LMS wave functions (~ 0 – 5%). These wave functions are of sufficient accuracy for the purposes of this investigation.

In Fig. 1 we present the calculations for the differential cross section of 604-eV electrons, as a function of the squared momentum transfer (in atomic units), and compare them with the two data points that exist at this energy.⁷ We see that

TABLE II. Parameters in the $1S$ and 2^1S helium wave functions Eqs. (2.11) and (2.12). Atomic units are used throughout.

Wave functions	N_i^2	Z_1	Z_2	c	N_f^2	Z_3	Z_4	c'
LMS	2.203	1.455 799	$2Z_1$	0.600	0.637	1.136	0.464	0.283 263
BJB	1.697	1.41	2.61	0.799	0.644	1.136	0.464	0.280 624
BJF	1.697	1.41	2.61	0.799	0.706	1.1946	0.4733	0.268 32

the present calculations (the lower three curves) are in good agreement with the data, whereas the Born calculations (the upper three curves) do poorly. Since the Born approximation appears to fail at this rather high energy, it would seem unlikely that it will be reliable at lower energies. However, the uncertainties in the data were not given in Ref. 7 and the range of $(a_0 q)^2$ over which the measurements were made (0.788–1.002) is quite small. More extensive tests are needed to conclusively distinguish between the two calculations.

In Fig. 2 are presented the calculations for the differential cross sections of 500-eV electrons which are compared with the data^{7,8} at or near this energy. The data in this energy region cover a range of q^2 values between $\sim 2 \times 10^{-2}$ and ~ 2.5 (in atomic units). The qualitative features of our calculations bear a striking resemblance to those we obtained for e -He elastic scattering at 500 eV.¹ In particular, at the larger momentum transfers

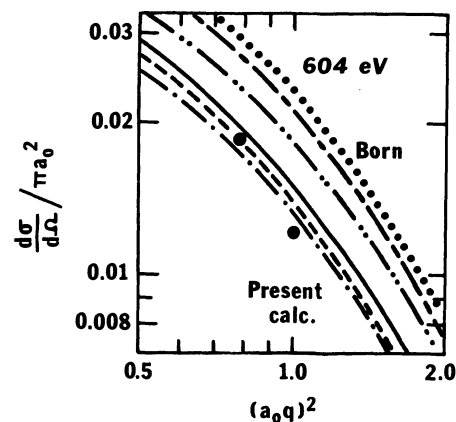


FIG. 1. Differential cross sections for e -He $1S$ - 2^1S transitions at 604 eV as a function of squared momentum transfer (in atomic units). The two measurements, represented by the solid circles, were made by Lassetre *et al.* (Ref. 7). The curves in the Born-approximation calculations and in the present calculations each employ three different pairs of ground-state and excited-state wave functions. In each calculation the uppermost of the three curves uses the BJF wave functions (see text and Table I for a fuller description of the wave functions), the middle curve uses the BJB wave functions, and the lower curve uses the LMS wave functions.

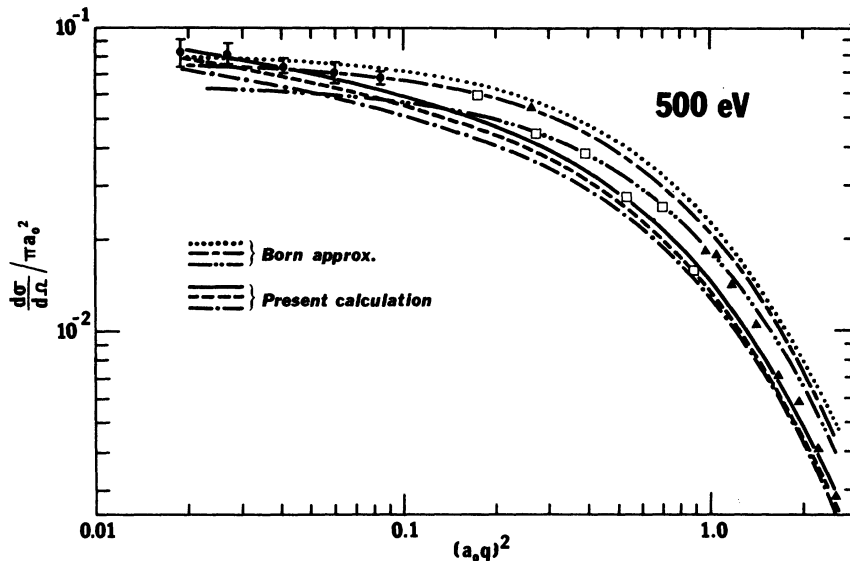


FIG. 2. Differential cross sections for e -He $1S$ - 2^1S transitions at 500 eV as a function of squared momentum transfer. The measurements, represented by the circles, squares, and triangles, were made, respectively, by Skerbele *et al.* (Ref. 8), Lassetre *et al.* (Ref. 7), and Silverman *et al.* (Ref. 7). The curves are as in Fig. 1. The measurements of Lassetre *et al.* (Ref. 7) were made at 511 eV.

shown the Born-approximation cross sections exceed the present Glauber calculations. At very small momentum transfers, the calculated intensities exceed the Born intensities since the differential cross sections continue to increase with decreasing q , whereas the Born cross sections approach constants as q is formally allowed to decrease toward zero. It is interesting to note that for e -He elastic scattering, the differential cross sections for the Born and Glauber approximations intersect near $(a_0q)^2 \approx 1$, whereas for the $1S$ - 2^1S transition they intersect near $(a_0q)^2 \approx 0.03$. Consequently there will be a much larger angular

region over which the $1S$ - 2^1S angular distribution in the Born approximation exceeds that in the Glauber approximation than was the case for elastic scattering.

The three different sets of wave functions pro-

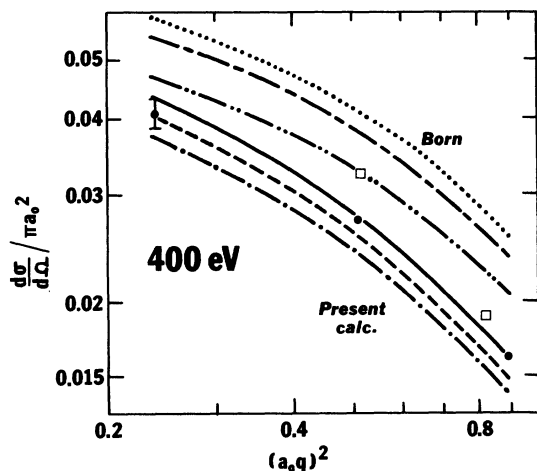


FIG. 3. Differential cross sections for e -He $1S$ - 2^1S transitions at or near 400 eV as a function of squared momentum transfer. The circles represent measurements by Chamberlain *et al.* (Ref. 5) and Vriens *et al.* (Ref. 9) at 400 eV. The squares represent measurements by Lassetre *et al.* (Ref. 7) at 417 eV. The curves are as in Fig. 1.

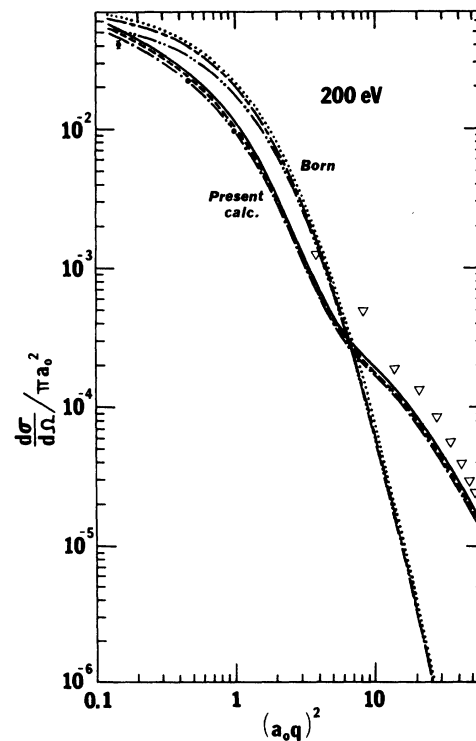


FIG. 4. Differential cross sections for e -He $1S$ - 2^1S transitions at 200 eV as a function of squared momentum transfer. The circles represent measurements by Chamberlain *et al.* (Ref. 5) and Vriens *et al.* (Ref. 9). The triangles represent measurements by Opal and Beaty (Ref. 11). The curves are as in Fig. 1.

duce no qualitative difference in the results. This is not unexpected since the general forms of the different wave functions used were identical. In Fig. 2 and in subsequent figures the experimental uncertainties are shown whenever such information has explicitly been published or provided to us by the experimenters.

The Born and Glauber calculations at 500 eV are both in qualitative agreement with the data. The two sets of data at the larger angles [$(a_0q)^2 \geq 0.2$] do not, themselves, appear to be in agreement with each other to within better than $\sim 20\%$. It is perhaps significant that of the six calculations shown, the BJF results of the Glauber approximation agree best with the data in both the small and large momentum transfer regions.

In Fig. 3 we see the calculations for the differential cross sections of 400-eV electrons and compare them with the data^{5,9} at 400 eV and the data⁷ at 417 eV. The data do not appear to be consistent near $(a_0q)^2 \approx 0.5$. With the exception of the 417-eV data point near $(a_0q)^2 \approx 0.5$, we note that the present calculations are superior to the

Born results, and the BJF Glauber results are in excellent agreement with the measurements.

In Fig. 4 we compare the calculations and data at 200 eV. The present calculations are in good agreement with the data^{5,9} at the smaller momentum transfers, $(a_0q)^2 \lesssim 1$. Also included in this figure are the data of Opal and Beaty¹¹ which extend out to very large momentum transfers, $(a_0q)^2 \approx 50$. These data were normalized¹¹ to other measurements. The magnitudes of the uncertainties in the absolute normalizations are not known well. The absolute value of the cross section near $(a_0q)^2 \approx 50$ may be in error by a factor of 2.¹¹ (The ratio of the $1S-2^1S$ to the $1S-2^1P$ measured cross sections is probably accurate to 15%.) The agreement of the present calculation with the data at large q is surprisingly good, whereas the Born-approximation result is orders of magnitude too small. The shoulder which seems to appear in the data near $(a_0q)^2 \approx 10$ is reproduced in our calculations. These data and calculations are evidence of structure in $d\sigma/d\Omega$ at the relatively high energy of 200 eV and large value of q .

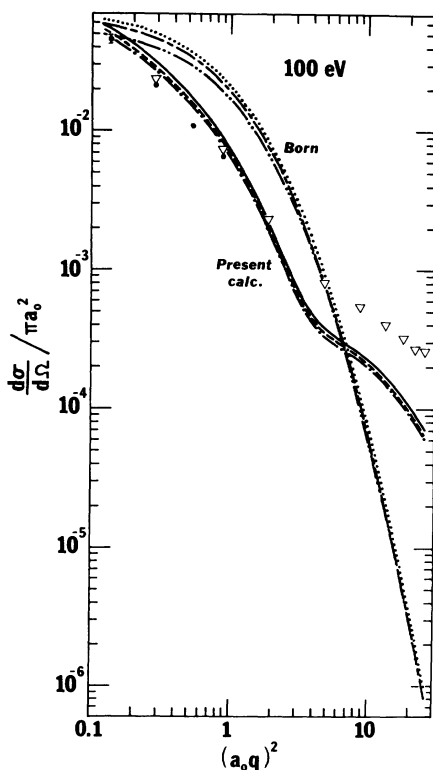


FIG. 5. Differential cross sections for e -He $1S-2^1S$ transitions at 100 eV as a function of squared momentum transfer. The circles represent measurements by Chamberlain *et al.* (Ref. 5) and Vriens *et al.* (Ref. 9). The triangles represent measurements by Crooks and Rudd (Ref. 12). The curves are as in Fig. 1.

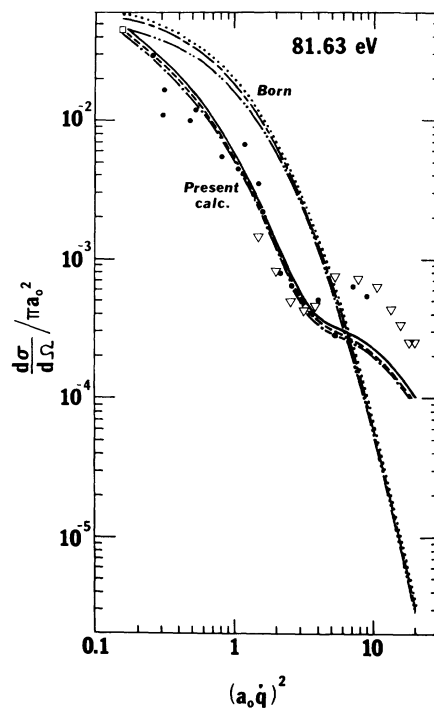


FIG. 6. Differential cross sections for e -He $1S-2^1S$ transitions at 81.63 eV as a function of squared momentum transfer. The circles represent measurements by Rice *et al.* (Ref. 10) at 81.63 eV. The triangles represent measurements by Opal and Beaty (Ref. 11) at 82 eV. The square represents a measurement by Chamberlain *et al.* (Ref. 5) at 75 eV. The curves correspond to 81.63-eV electrons and are as described for Fig. 1.

In Fig. 5 the data^{5,9,12} and calculations for 100-eV electrons are shown. These data include the high-momentum-transfer measurements of Ref. 12 ($a_0^2 q^2 \lesssim 25$). The present calculations are in agreement with the data in the region $0.1 < (a_0 q)^2 < 2$. In this region the Born approximation is typically too high by a factor of ~ 2 . For $a_0^2 q^2 \gtrsim 4$ the present calculations are in qualitative agreement with the data, exhibiting a much slower decrease of $d\sigma/d\Omega$ with q^2 similar to that shown by the data. Quantitatively the present calculations are too low by a factor of ~ 3 in this region. At the highest momentum transfer ($a_0^2 q^2 \approx 25$) the Born approximation, on the other hand, is too low by a factor of ~ 300 .

In Fig. 6 the calculations and data^{5,10,11} for 82-eV electrons are compared. The data include the high-momentum-transfer measurements of Refs. 10 and 11 and contain interesting structure. The qualitative difference between the 100-eV data shown in Fig. 9 and the 82-eV data in this figure is rather marked. The present calculations are in good agreement with the data in the region $(a_0 q)^2 \lesssim 4$. Near $(a_0 q)^2 = 4$, the measured value of $d\sigma/d\Omega$ attains a minimum. The present cal-

culations cannot reproduce this minimum and the subsequent maximum. The theory does, however, give rise to a rather pronounced shoulder which results in a cross section that is too low by "only" a factor of ~ 2.5 in the region $7 \lesssim (a_0 q)^2 \lesssim 20$. On the other hand, at $(a_0 q)^2 \approx 20$ the Born approximation is too low by a factor of ~ 80 and appears to be getting even worse. Thus the Glauber theory apparently contains the ingredients for reproducing the observed structure, but it does not yield quite enough of it.

In Fig. 7 we again see structure in the data¹² which are for 50-eV electrons. The theory does well in the region $(a_0 q)^2 \lesssim 2$. It fails, however, to reproduce the rather sharp minimum of the data. Nevertheless it is apparent that in the region where the measured cross section increases with increasing q , the theoretical predictions yield a minimum in the cross section, albeit a very shallow one. The mechanism responsible for the increase in the measured values of $d\sigma/d\Omega$ are presumably being taken into account to some extent by the theory.

The appearance of the minimum in the cross section is suggestive of the minima that appear in cross sections for scattering of hadrons by light nuclei. There the minima and maxima can be interpreted in terms of multiple-scattering phenomena.²⁹ Although one might at first think that nothing is to be gained by referring to nuclear physics, where the basic interactions are rather different from those in electron-atom collisions, a little thought will reveal quite a close qualitative similarity between the atomic and nuclear cases when dealing with *composite* systems. For example, scattering of high-energy hadrons by light nuclei characteristically reveals minima and maxima. These are explained by the Glauber theory in terms of multiple scattering. As a simple example, consider hadron-deuteron collisions. In Glauber theory the scattering amplitude consists of an amplitude for single scattering plus one for double scattering. The single-scattering amplitude corresponds to single scattering by the constituent nucleons. It contains the hadron-nucleon amplitude as a factor, is rather large in the forward direction, and decreases quite rapidly with increasing momentum transfer q . The double-scattering amplitude is rather small in the forward direction but decreases quite slowly with increasing q and eventually dominates the single-scattering amplitude. In the region where the two amplitudes are comparable, there is significant interference between them and a minimum or shoulder appears in the differential cross section.

Precisely the same kind of analysis is applicable in the Glauber theory of electron-atom collisions.

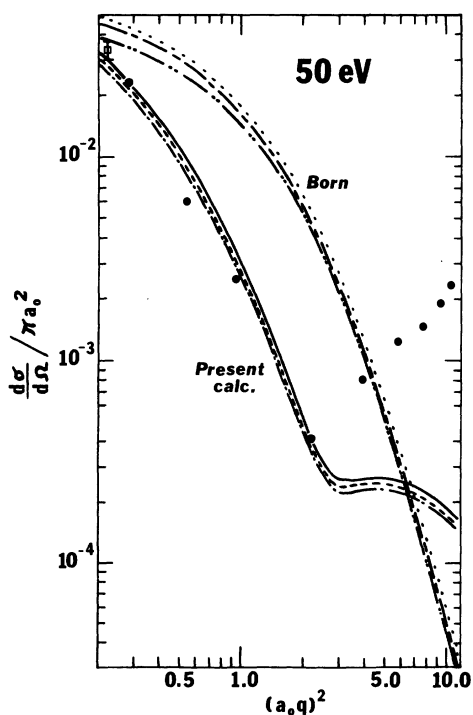


FIG. 7. Differential cross sections for e -He $1S$ - 2^1S transitions at 50 eV as a function of squared momentum transfer. The circles represent measurements by Crooks and Rudd (Ref. 12) and the square represents a measurement by Chamberlain *et al.* (Ref. 5). The curves are as in Fig. 1.

There it is convenient to take the amplitude for scattering by the *neutral hydrogen atom* to be the basic amplitude (rather than the amplitude between the electron and a single charged particle). One can then express the e -He scattering amplitude as a single-scattering amplitude plus a double-scattering amplitude. The single-scattering amplitude corresponds to scattering of the incident electron by neutral systems consisting of a single electron bound to a massive positive singly charged core. (The helium atom will be thought of as two such systems bound together.) This single-scattering amplitude can be calculated analytically and has the requisite feature that it is large near the forward direction and decreases quite rapidly with increasing q . The remaining double-scattering amplitude is smaller near the forward direction, but may decrease less rapidly with increasing q and may eventually dominate over the single-scattering amplitude. In the region where the two amplitudes are comparable, there is significant interference between them and a minimum or shoulder may appear in the differential cross section. Furthermore, in the region where double scattering dominates, the

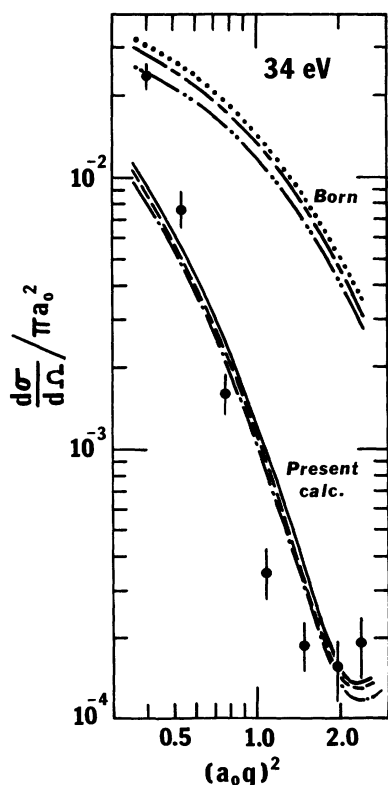


FIG. 8. Differential cross-sections for e -He $1S-2^1S$ transitions at 34 eV as a function of squared momentum transfer. The measurements are by Rice *et al.* (Ref. 10). The curves are as in Fig. 1.

cross sections would possess the characteristics of the double-scattering amplitude such as a very slow decrease or a shoulder.

The qualitative features of the single- and double-scattering amplitudes just described do in fact appear in e -He scattering at energies where the theoretical cross sections reveal minima. For example, for 50-eV electrons, calculations we have performed show that the single-scattering term dominates for $q^2 < 3$. At $q^2 \approx 3$ the double-scattering term becomes dominant. Reference to Fig. 7 shows that $q^2 \approx 3$ is indeed the region of the mini-

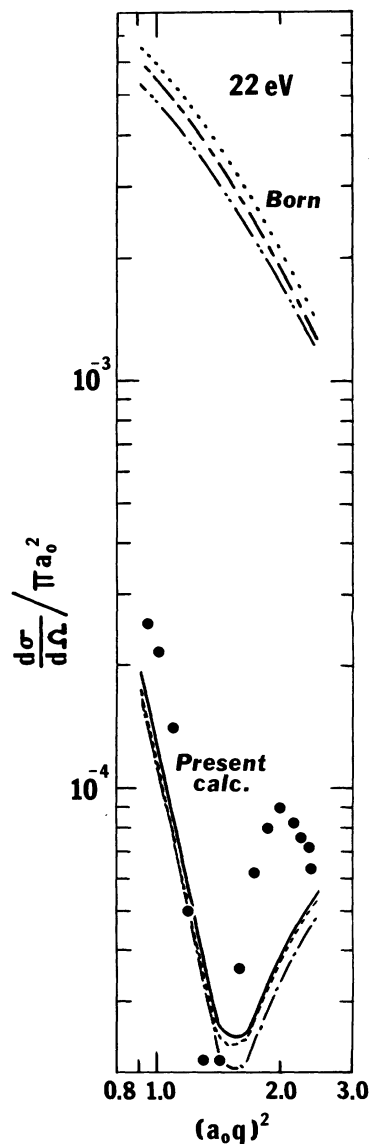


FIG. 9. Differential cross sections for e -He $1S-2^1S$ transitions at 22 eV as a function of squared momentum transfer. The unnormalized measurements, by Andrick *et al.* (Ref. 30), have been arbitrarily normalized to the theory at $(a_0q)^2 \approx 1.2$. The curves are as in Fig. 1.

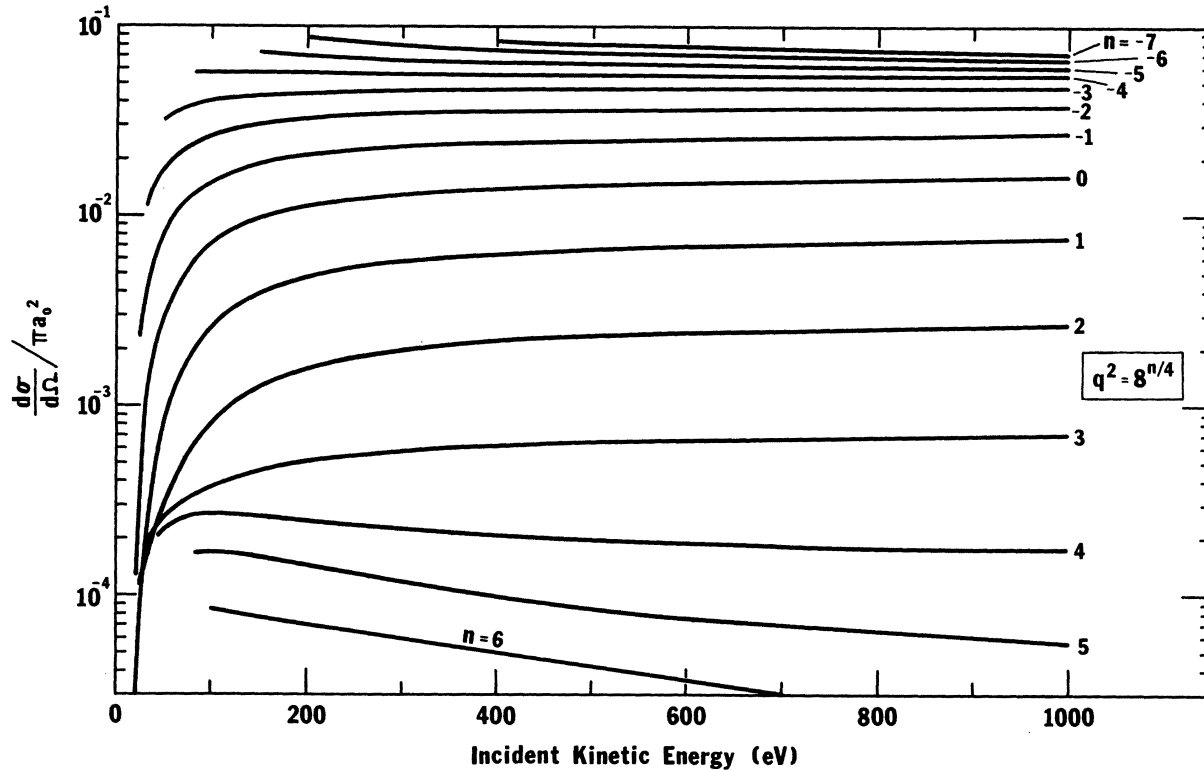


FIG. 10. Differential cross sections for e -He $1S$ - 2^1S transitions for various fixed values of q^2 , as a function of the incident kinetic energy. The values of q^2 are given by $q^2 = 8^{n/4}$, where n is an integer ranging from -7 to 6 . Each curve is labeled by its value of n .

imum in the differential cross section. Furthermore, it is a shallow minimum because for $3 \lesssim q^2 \lesssim 6$ the dominant double-scattering term is practically constant.

Although the Glauber approximation is regarded as a high-energy approximation, it is not clear what the lower limit to the energy must be for validity of the theory. Studies of e -H scattering indicate that the theory may be useful at energies considerably below 50 eV. Furthermore, in nuclear physics it has been found that Glauber theory works at rather low energies, even near resonances. For these reasons we present comparisons of the theory with some of the data below 50 eV.

As the incident energy is decreased, the theoretical minimum becomes deeper and sharper. This is exhibited in Figs. 8 and 9 where the data^{10,30} at 34 and 22 eV are compared with the calculations.

In Fig. 8 (34 eV) it is interesting to note that the theory predicts the correct value for the minimum, and the prediction of its position ($q^2 \approx 2.3$) is quite close to the measured value ($q^2 \approx 2.0$).

In Fig. 9 the data of Ref. 30 are compared with the calculations. Since the data given were un-

normalized, we have arbitrarily normalized them to the theory at $q^2 \approx 1.2$. Our predicted minimum occurs near $q^2 \approx 1.5$ and the measured value occurs near $q^2 \approx 1.35$. The measurements also show a sharp maximum near $q^2 \approx 2$ which the theory does not reproduce.

It should be pointed out that the calculations neglect exchange effects, as have all previous Glauber-approximation calculations. These effects should be non-negligible at the lowest energies. It is possible that the quantitative discrepancies between the data and the calculations below 50 eV arise not from the basic Glauber approximation but from the neglect of exchange effects (which are very difficult to calculate in the Glauber approximation).

We have compared calculations similar to those we have shown, with the data at 300, 225, 175, 150, 55.5, 44, and 26.5 eV. The results are qualitatively the same as those shown in Figs. 1-9.

In Fig. 10 we show the scattered intensity as a function of incident energy for various fixed values of q^2 . This figure shows the qualitative results of our calculations at a glance. Minima and maxima in angular distributions occur whenever crossovers appear in the curves. Inflection

points can also be determined from this figure by measuring the vertical distance between successive curves.

We have seen that the general methods of Ref. 21 may be applied without difficulty to the $1S-2^1S$ transition in helium. The application has included a rather wide range of incident energies, from 22 to 600 eV, and a rather wide range of momentum transfers, from $q^2 \approx 0.02$ to $q^2 \approx 50$. In addition to exhibiting the utility of the methods of Ref. 21, our numerical results have extended beyond those of Ref. 20 in regard to incident energy and momentum transfer. In some cases, such as the 200-eV case, the new results have shown that our methods yield relatively good results even at rather large momentum transfers. This is in contrast, for example, to a recent high-energy approximation³¹ where the discrep-

ancy between theory and experiment is a factor of approximately 4. The methods of Ref. 21 may be used in calculating other transitions in helium and elastic and inelastic scattering by other atoms. The demonstrated utility of these methods will enable more extensive tests of the application of the Glauber approximation to atomic physics.

ACKNOWLEDGMENTS

The author wishes to thank Dr. G. B. Crooks and Dr. J. Rice for providing him with measurements prior to publication. He also thanks Dr. G. E. Chamberlain, Dr. E. N. Lassetre, Dr. C. B. Opal, and Dr. A. Skerbele for discussions concerning their measurements and for more detailed descriptions of the data than do appear in the literature.

*Supported in part by the National Science Foundation and by the City University of New York Faculty Research Award Program.

¹V. Franco, *Phys. Rev. A* **1**, 1705 (1970).

²V. Franco, *Phys. Rev. Lett.* **20**, 709 (1968).

³V. Franco and B. K. Thomas, *Phys. Rev. A* **4**, 945 (1971); and *Bull. Am. Phys. Soc.* **15**, 1504 (1970).

⁴L. Vriens, C. E. Kuyatt, and S. R. Mielczarek, *Phys. Rev.* **170**, 163 (1968).

⁵G. E. Chamberlain, S. R. Mielczarek, and C. E. Kuyatt, *Phys. Rev. A* **2**, 1905 (1970); G. E. Chamberlain (private communication).

⁶J. P. Bromberg, *J. Chem. Phys.* **50**, 3906 (1969).

⁷E. N. Lassetre, M. E. Krasnow, and S. Silverman, *J. Chem. Phys.* **40**, 1242 (1964); S. M. Silverman and E. N. Lassetre, *J. Chem. Phys.* **40**, 1265 (1964).

⁸A. Skerbele and E. N. Lassetre, *J. Chem. Phys.* **45**, 1077 (1966); A. Skerbele (private communication).

⁹L. Vriens, A. Simpson, and S. R. Mielczarek, *Phys. Rev.* **165**, 7 (1968).

¹⁰J. R. Rice, D. G. Truhlar, D. C. Cartwright, and S. Trajmar, *Phys. Rev. A* **5**, 762 (1972); J. Rice (private communication).

¹¹C. B. Opal and E. C. Beaty, *J. Phys. B* **5**, 627 (1972); C. B. Opal (private communication).

¹²G. B. Crooks and M. E. Rudd, *Bull. Am. Phys. Soc.* **17**, 131 (1972); G. B. Crooks (private communication).

¹³Y.-K. Kim and M. Inokuti, *Phys. Rev.* **175**, 176 (1968); K. L. Bell, D. J. Kennedy, and A. E. Kingston, *J. Phys. B* **2**, 26 (1969).

¹⁴E. N. Lassetre, *J. Chem. Phys.* **53**, 3801 (1970).

¹⁵R. J. Glauber, in *Lectures in Theoretical Physics*, edited by W. E. Brittin *et al.* (Interscience, New York, 1959), Vol. I.

¹⁶H. Tai, P. J. Teubner, and R. H. Bassel, *Phys. Rev. Lett.* **22**, 1415 (1969); *Phys. Rev. Lett.* **23**, 453(E) (1969).

¹⁷H. Tai, R. H. Bassel, E. Gerjuoy, and V. Franco, *Phys. Rev. A* **1**, 1819 (1970).

¹⁸A. S. Ghosh, P. Sinha, and N. C. Sil, *J. Phys. B* **2**, L58 (1970).

¹⁹B. K. Thomas and E. Gerjuoy, *J. Math. Phys.* **12**, 1567 (1971).

²⁰A. C. Yates and A. Tenney, *Phys. Rev. A* **6**, 1451 (1972).

²¹V. Franco, *Phys. Rev. Lett.* **26**, 1088 (1971).

²²P.-O. Löwdin, *Phys. Rev.* **90**, 120 (1953).

²³R. Marriott and M. J. Seaton, *Proc. Phys. Soc. Lond.* **70**, 296 (1957).

²⁴F. W. Byron, Jr. and C. J. Joachain, *Phys. Rev.* **146**, 1 (1966).

²⁵C. C. J. Roothaan, L. M. Sachs, and A. M. Weiss, *Rev. Mod. Phys.* **32**, 186 (1960).

²⁶J. van den Bos, *Phys. Rev.* **181**, 191 (1969).

²⁷M. R. Flannery, *J. Phys. B* **3**, 306 (1970).

²⁸M. Cohen and R. P. McEachran, *Proc. Phys. Soc. Lond.* **92**, 37 (1967).

²⁹See, for example, V. Franco and E. Coleman, *Phys. Rev. Lett.* **17**, 827 (1966).

³⁰D. Andrick, H. Ehrhardt, and M. Eyb, *Z. Phys.* **214**, 388 (1968).

³¹M. B. Hidalgo and S. Geltman, *J. Phys. B* **5**, 617 (1972).